Supporting Information

Magnetic Archimedean Tessellations in Metal-Organic Frameworks

Hua Chen,[†] Laura Voigt,[†] Mariusz Kubus,[†] Dmytro Mihrin,[†] Susanne Mossin,[†] René Wugt Larsen,[†] Søren Kegnæs,[†] Stergios Piligkos,[‡] Kasper S. Pedersen[†]

† Department of Chemistry, Technical University of Denmark, Kemitorvet, Building 207, DK-2800 Kgs. Lyngby, Denmark

‡ Department of Chemistry, University of Copenhagen, DK-2100 Copenhagen, Denmark

Journal of the American Chemical Society

Materials and Methods

All procedures were carried out in an InertLab glovebox under a dry Ar atmosphere. Elemental analysis was performed by the Mikroanalytisches Laboratorium Kolbe (Oberhausen, Germany). GdI_3 (99.99%) and DyI_3 (99.99%) were supplied by Alfa Aesar, and sodium and 4,4′-bipyridine (bipy; 98%) were supplied by Sigma-Aldrich. All reagents were used as received. Dry and oxygen-free solvents were obtained from a Puresolv MD 7 solvent purification system.

Synthesis

Gd: Powdered GdI_3 (135 mg, 250 μmol) and acetonitrile (14 mL) were stirred vigorously for 30 min. An acetonitrile solution (7 mL) of 4,4′-bipyridine (195 mg, 1.25 mmol) and sodium metal (5.8 mg, 250 μmol) was added dropwise to the GdI_3 suspension with stirring. A dark blue microcrystalline powder formed immediately. The mixture was left stirring for 10 min. The solid material isolated by suction filtration and washed with cold acetonitrile (–20 °C; 2 ×10 mL). Yield: 90 mg (45%). Anal. calcd. (found) for $C_{27}H_{23}GdI_2N_6$ (corresponding to $GdI_2(bipy)_{5/2}{\cdot}CH_3CN$): C, 38.5 (38.2); H, 2.73 (2.81); N, 9.98 (9.91); I, 30.2 (29.7); Gd, 18.7 (18.3). Dark-blue single-crystals suitable for single-crystal X-ray diffractometry were obtained by slow diffusion. Powdered GdI_3 (135 mg, 250 μmol) was placed at the bottom of a glass test tube (160 ×16 mm) and carefully covered by acetonitrile (14 mL). The $Na^+(bipy^{\bullet-})$/bipy solution (prepared as above) was gently layered on the top and the covered test tube was kept in the fridge (–20 °C) for 14 days. **Gd′** formed as a trace byproduct phase. **Dy**: The synthesis of **Dy** is identical to that of **Gd** but employs DyI_3. Single-crystals of **Dy** are grown similarly to **Gd**. Yield: 86 mg (43%). Anal. calcd. (found) for $C_{27}H_{23}DyI_2N_6$ (corresponding to $DyI_2(bipy)_{5/2}{\cdot}CH_3CN$): C, 38.2 (38.1); H, 2.73 (2.76); N, 9.91 (9.87); I, 29.9 (29.9); Dy, 19.2 (19.3).

EPR spectroscopy

EPR spectra of both solid samples and frozen solutions were obtained at 77 K on a Bruker EMX X-band EPR spectrometer (rectangular cavity ST4102) fitted with a small Dewar for liquid nitrogen. The experimental parameters for the frozen solution of a freshly made solution of $Na^+(bipy^{\bullet-})$ were: Microwave frequency 9.52 GHz, power 0.42 mW, time constant 20 ms, field interval 338.5–340.5 mT, modulation frequency 100 kHz, amplitude 1.0 G. The observed line is very intense (Fig. S1) and narrow and can be simulated with a *g*-value of 2.0045 and a Lorentzian line shape (line width 0.15 mT). The EPR signal of **Gd** (Fig. S2) is very broad and spans the field

interval from 0–0.65 T. The parameters used for the solid sample were microwave frequency 9.52 GHz, power 6.6 mW, time constant 20 ms, field interval 42–642 mT, modulation frequency 100 kHz, amplitude 5 G.

X-ray diffraction

Single-crystals of **Gd**, **Gd′**, and **Dy** were immersed in polybutene oil (Aldrich, >90%) and mounted on a nylon loop, which was attached to a SuperNova Dual Source CCD-diffractometer. Data were collected using Cu Kα (λ = 1.5406 Å) radiation at 100(1) or 120(1) K. The structures were solved in Olex2[1] using the structure solution program olex2.solve 1.3[2] for **Gd**, **Dy**, and SHELXT 2018/2[3] for **Gd′** and subsequently refined with the SHELXL[4] refinement package using least squares minimization. All non-hydrogen atoms were refined anisotropically. For both **Gd** and **Dy**, the structure was refined as an inversion twin with a BASF parameter of 0.501(7) and 0.44(1) respectively. In the **Dy** structure due to bipy disorder, the DFIX command was used to restrain distances in the aromatic ring with the N6 atom, and the SIMU and DELU commands were used to restraint the thermal parameters. Additionally, it was necessary to enforce ISOR restraints on the ADPs for the C25 atom and the equality constraints EADP on the ADPs of C24, C24A atom pair in the ring. Furthermore, the AFIX 66 command was used to maintain the geometry of the aromatic ring with the N4 atom. The restraint command SIMU was applied to the disordered C25, C24, and C24A atoms of the bipy molecule in the **Gd** structure. The geometry of the acetonitrile molecules in **Gd** and **Dy** was restrained using the DFIX, SIMU, and RIGU instruction (molecules imported from FragmentDB[5,6]). Additionally, ADPs of atoms in the acetonitrile molecules with N8, N10, N12, N13, N15 in the Dy structure and N11, N13, and N14 in the Gd structure were restrained to behave isotropically (ISOR).

The powder X-ray diffraction patterns were collected using Cu Kα (λ = 1.54056 Å) radiation in the range 6° < 2θ < 32°, with a 2θ step size of 0.01° using the SuperNova Dual Source CCD diffractometer. The diffraction pattern of **Dy** was collected at 296 K with an exposure time of 10 minutes. The XRD pattern of **Gd** was collected at 295 K with an exposure time of 30 minutes. The samples were loaded in a capillary glass tube with a 0.3 mm outer diameter and a 0.01 mm wall thickness, and rotated during the measurements.

Table S1. Crystallographic data and refinement parameters.

Compound	**Gd**	**Gd′**	**Dy**
CCDC number	2064815	2064816	2064814
Temperature / K	120	100	120
Crystal system	Tetragonal	Triclinic	Tetragonal
Space group	$I4_122$	$P\bar{1}$	$I4_122$
a / Å	23.2431(4)	9.1899(4)	23.1474(5)
b / Å	23.2431(4)	12.0151(5)	23.1474(5)
c / Å	33.3715(7)	14.4033(4)	33.2433(8)
α / °	90	97.498(3)	90
β / °	90	93.432(3)	90
γ / °	90	95.807(4)	90
Volume / Å^3	18028.7(7)	1564.4(1)	17811.8(8)
Z	16	2	16
ρ_{calc} / g cm^{-3}	1.447	1.702	1.473
μ / mm^{-1}	20.52	29.34	20.11
Radiation	Cu Kα (λ = 1.54184 Å)	Cu Kα (λ = 1.54184 Å)	Cu Kα (λ = 1.54184 Å)
2θ range for data collection / °	7.55–151.57	7.47–127.37	7.58–127.37
Index ranges	$-29 \le h \le 27$	$-10 \le h \le 10$	$-16 \le h \le 26$
	$-25 \le k \le 19$	$-13 \le k \le 13$	$-26 \le k \le 23$
	$-41 \le l \le 41$	$-15 \le l \le 16$	$-36 \le l \le 38$
Reflections collected	34231	13903	25778
Independent reflections	9226 [R_{int} = 0.073]	5130 [R_{int} = 0.141]	7335 [R_{int} = 0.058]
Data/restraints/parameters	9226/275/555	5130/0/298	7335/360/537
Goodness-of-fit on F^2	1.03	1.05	1.04
Final R_1 index [$F^2 \ge 2\sigma(F^2)$]	0.051	0.10	0.049
Final wR_2 index [F^2]	0.15	0.27	0.14
Largest diff. peak/hole / e Å^{-3}	1.00/–1.65	3.68/–3.53	1.01/–1.94

Magnetometry

Direct current (dc) magnetization measurements were performed using the VSM option of a QuantumDesign Dynacool Physical Property Measurement System (PPMS) equipped with a 9 T superconducting magnet in between 1.7 K and 273 K. The polycrystalline samples were loaded into standard QuantumDesign powder capsules inside an Ar-filled glovebox, sealed with wax, and mounted in a standard brass sample holder. The sample holder was transferred air-tight to the PPMS chamber and the sample space was immediately evacuated and purged with He. The experimental magnetization data were corrected for diamagnetic contributions from the sample holder and the intrinsic sample diamagnetism. Alternating current (ac) magnetization data were acquired using the ACMS-II option (10–10,000 Hz, $H_{ac} \leq 16$ Oe) and on polycrystalline samples immobilized in polycarbonate capsules mounted in plastic drinking straws and handled as above. The paramagnetic relaxation times were extracted from the maxima of the $\chi''(\nu_{ac})$ data as $\tau^{-1} = 2\pi\nu_{ac}$.

Modelling of the magnetic properties of **Gd** was performed within the framework of the phenomenological spin-Hamiltonian formalism. Given that **Gd** can be considered as an eight-member ring made by alternating Gd(III) and bipy$^{\bullet-}$ and since both these species are relatively magnetically isotropic the simplest general form of spin-Hamiltonian ($\widehat{H}$, Eq. 1, main text) appropriate for the phenomenological description of the magnetic properties of **Gd** should only contain terms expressing the isotropic magnetic exchange interaction between the constitutive centers and the isotropic response of the system to an external magnetic field according to the Zeeman interaction. The dimension, N, of the square matrix corresponding to the matrix representation of $\widehat{H}$ for **Gd** is:

$$N = \prod_i^n (2S_i + 1) \qquad \text{Eq. S1}$$

resulting in $N = 8^4\ 2^4 = 65536$ for **Gd**. The magnitude of N precludes numerical diagonalization of the full spin-Hamiltonian matrix by conventional approaches[1] because of unrealistic computer memory and processor time requirements. Within the Irreducible Tensor Operator (ITO) formalism,[7] the isotropic exchange parameter, J_{ij}, is associated to a tensor operator $\hat{O}_q^K$ of order $K = 0$ and thus, necessarily of projection $q = 0$ ($-K \leq q \leq K$, with K and q integers), since it is associated to the scalar product, $\hat{S}_i \cdot \hat{S}_j$, of the Cartesian spin-operators. The matrix elements of a tensor operator $\hat{O}_q^K$ within the coupled total spin, S, basis $|s, S, M_S\rangle$ is given by:

$$\langle s, S, M_S | \hat{O}(k, K, q) | s', S', M_S' \rangle = (-1)^{S-M_S} \begin{pmatrix} S & K & S' \\ -M_S & q & M_S' \end{pmatrix} \langle s, S \| k, K \| s', S' \rangle \qquad \text{Eq. S2}$$

where s, s' and k are all necessary additional quantum numbers to fully define the problem, M_S is the projection of S along the quantization axis, the first term of the right-hand side is a phase, the second one is a 3-j symbol and the third is a reduced matrix element, independent of M_S. For the 3-j symbol to be non-zero a) the triangle relation has to hold for S, K and S', from where $S = S'$, since $K = 0$; and b) $M_S' - M_S = q$, has to hold. Thus, the isotropic exchange interaction has non-zero matrix elements only between basis-function of the same total spin S. Furthermore, since for the isotropic exchange associated tensor operator $\hat{O}_q^K$, $q = 0$, the matrix element of Eq. S2 is independent of M_S, to a phase factor of ±1 which is irrelevant for the computation of eigenvalues. Thus, only one of the $2S+1$ projections of each total S multiplet is necessary to be included into this block-diagonal form of $\hat{H}_{iso}$, since the information contained in the $2S$ others is redundant. Finally, since $\hat{S}^2$ commutes with $\hat{S}_z$, $\hat{S}^2$ and $\hat{S}_z$ have a simultaneous eigenbasis specified by their respective eigenvalues S and M_S. This allows to transform the matrix representation of $\hat{H}$ for **Gd** into block-diagonal form, where each block corresponds to basis-functions of the same total spin S and projection M_S. Use of this methodology allows to transform the matrix representation of $\hat{H}$ for **Gd**, into block-diagonal form made up from seventeen blocks each corresponding to a total spin value S, ranging from 0 to 16, the dimensions of which are given below in Table S2.

Table S2. Total spin, S, and associated dimension, N_S, of the corresponding block in the block-diagonal form of the matrix representation of $\hat{H}$ for **Gd**.

S	N_S
16	1
15	7
14	24
13	56
12	104
11	168
10	248
9	344
8	452
7	556
6	632
5	664
4	648
3	584
2	472
1	312
0	110
sum	**5382**

The dimensions of the block-diagonal form of the matrix representation of $\widehat{H}$ for **Gd** (Table S2) are compatible with standard numerical diagonalization approaches.[8] The number of independent isotropic magnetic exchange parameters that can, in principle, be included in $\widehat{H}$ is determined by the number of different super-exchange paths between the Gd(III) and and bipy$^{\bullet-}$ in **Gd**. Herein we assume a unique isotropic exchange parameter, J, since all superexchange paths are symmetry related. Additional exchange interactions originating from magnetic dipole interactions are neglected because they are usually much smaller in magnitude than the exchange interactions via bridging ligands, as they depend inversely to the cube of the intermetallic distance. Using J as a unique fit parameter allowed the temperature dependence of the χT product and the M vs H data of **Gd** to be simultaneously numerically fitted, by use of the Levenberg-Marquardt algorithm,[9] to the isotropic spin-Hamiltonian $\widehat{H}$. This resulted in the best fit parameters $J = 0.073(4)$ cm^{-1}. Under these conditions, the spin ground state of **Gd** is an $S = 12$ (Fig. S8), separated by the first excited state, a degenerate doublet of $S = 11$ states, by only 0.16 cm^{-1} at zero magnetic field.

NIR and MIR spectroscopy

The mid-IR and near-IR direct absorption spectra were collected by a VERTEX80v Fourier transform vacuum spectrometer from Bruker Optics GmbH. Highly air-sensitive samples of polycrystalline **Gd** were sandwiched between pairs of optically transparent KBr and CaF_2 windows for the mid-IR and near-IR recordings, respectively, and subsequently sealed effectively with silicone oil at the window edges in an argon-filled glove box. The FTIR apparatus was configured with a Ge on KBr beam splitter, a liquid N_2 cooled HgCdTe detector and a thermal globar radiation source for the mid-IR single-beam measurements collected with a spectral resolution of 2 cm^{-1}. The combination of a CaF_2 beam splitter, a liquid N_2 cooled InSb detector, and a thermal tungsten lamp source was employed for the near-IR single-beam measurements collected at a spectral resolution of 3 cm^{-1}. The resulting absorbance spectra were subsequently baseline-corrected slightly and minor traces of residual water vapor absorption were subtracted.

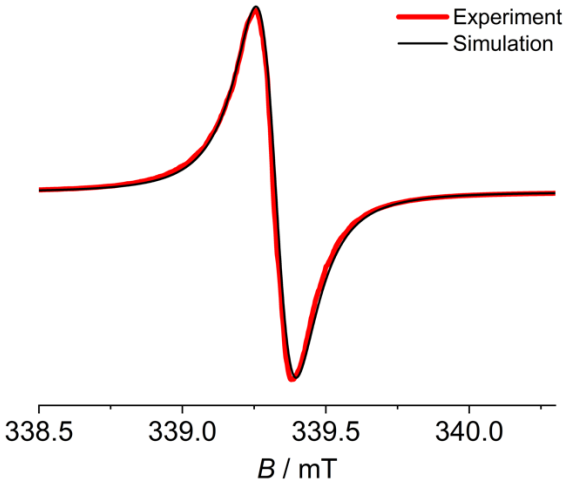

Fig. S1. Frozen-solution (CH_3CN) X-band (9.52 GHz) EPR spectrum at 77 K of the reaction product between one equivalent of Na metal and 2.5 mol equivalent of bipy, as described in the main text.

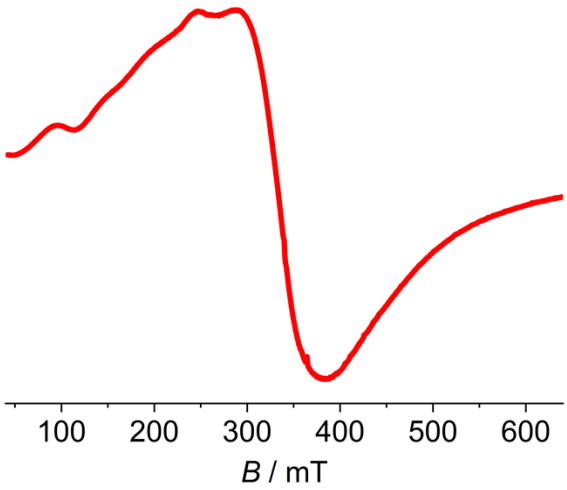

Fig. S2. X-band (9.52 GHz) EPR spectrum at 77 K of polycrystalline **Gd** obtained at 77 K.

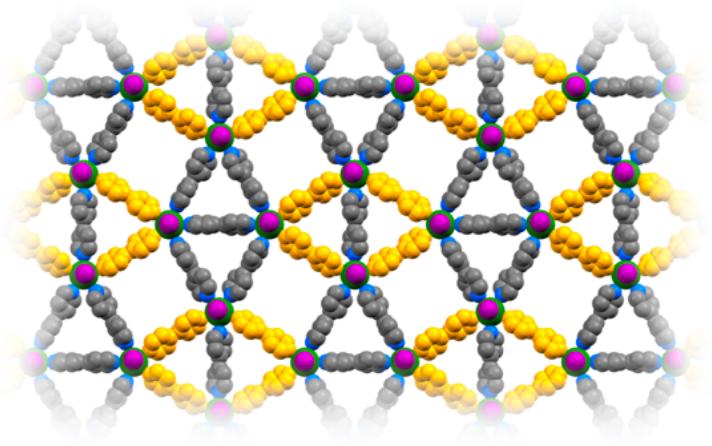

Fig. S3. Formation of $\{M^{III}_4(bipy^{\bullet-})_4\}$ rhombi in **Gd** and **Dy** as suggested by single-crystal X-ray diffraction analysis. Color code: $bipy^{\bullet-}$, yellow; $bipy^0$, grey.

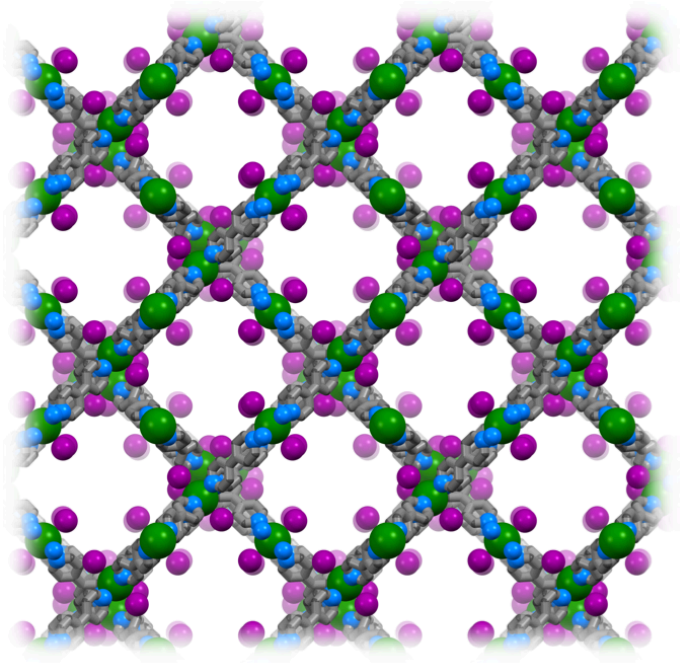

Fig. S4. Crystal structure of **Gd** shown along the crystallographic *c* axis showing the presence of interpenetrating 2D layers.

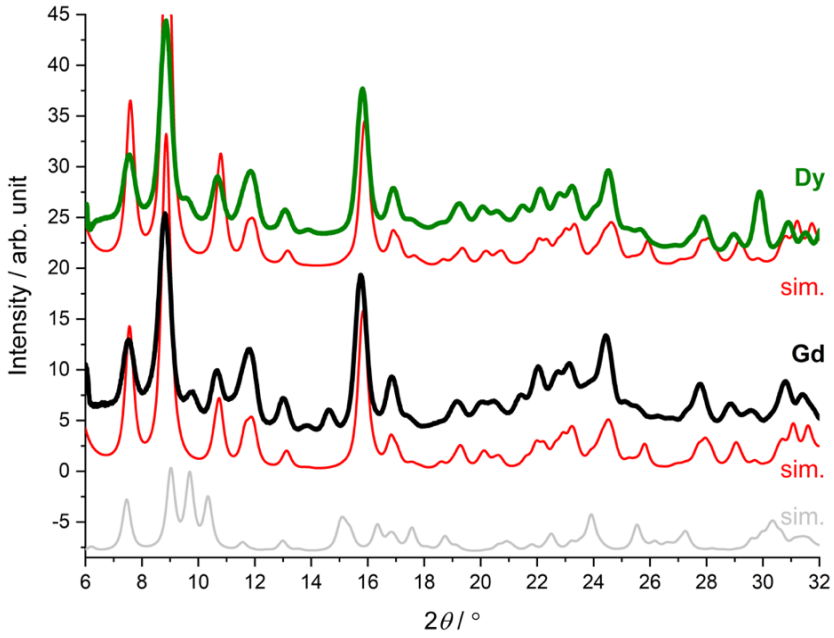

Fig. S5. Powder X-ray diffractograms of **Gd** and **Dy** and corresponding simulations from the 120-K single-crystal X-ray structures. The grey trace is a simulation of the powder diffractogram of **Gd′** (100 K).

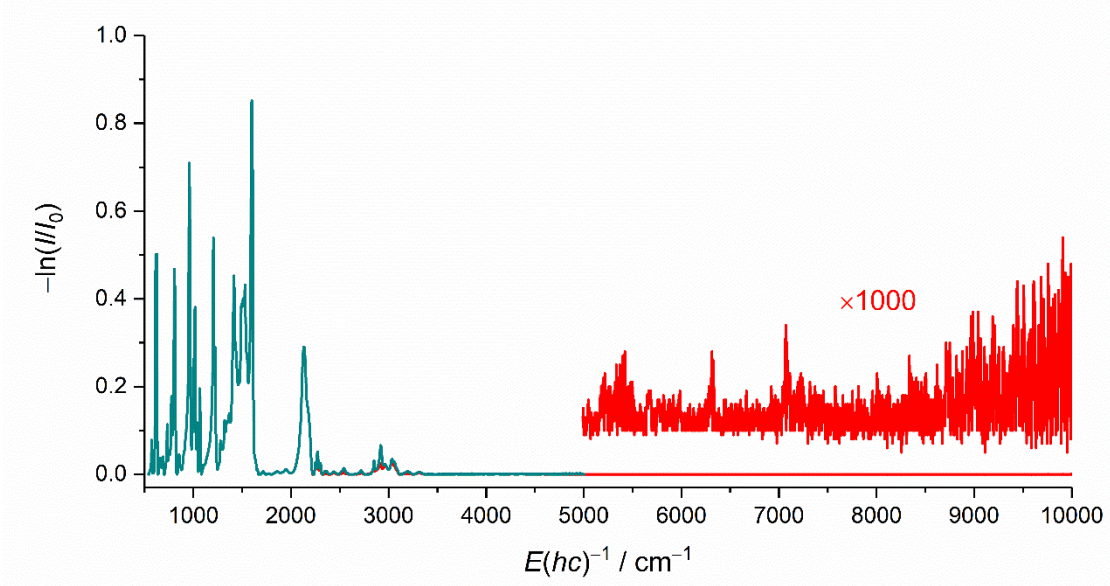

Fig. S6. Mid-IR/near-IR absorbance spectrum of polycrystalline **Gd** obtained at RT. The weak traces of gas-phase absorption lines around 5300–5400 cm^{-1} (combination of OH stretching fundamental + OH bending fundamental) and 7100-7200 cm^{-1} (first overtone of the OH stretching fundamental) comes from uncompensated water vapor absorption.

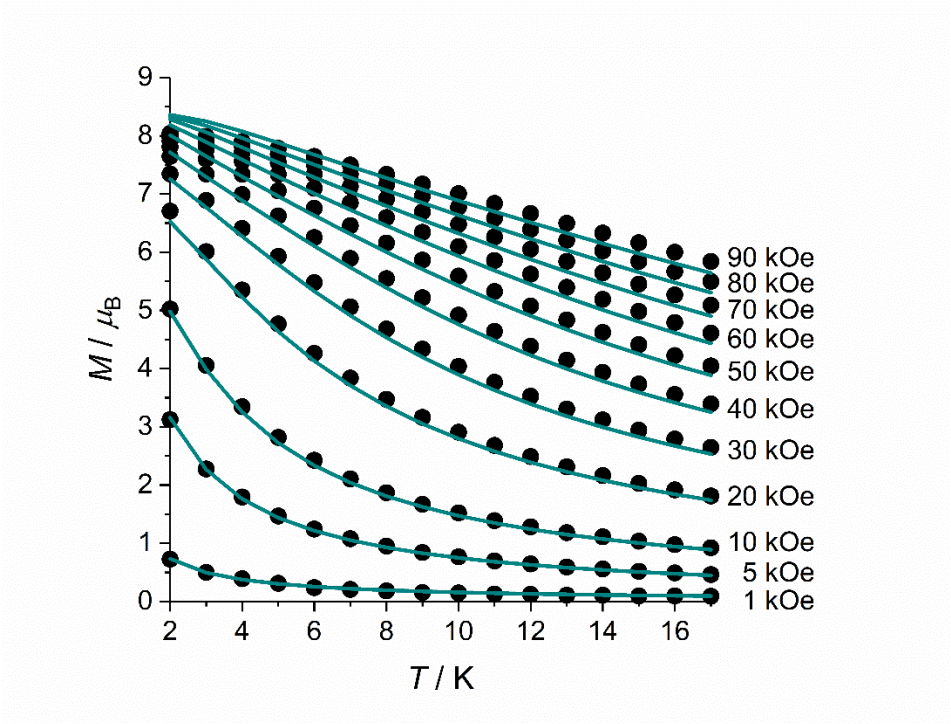

Fig. S7. Temperature dependence of the magnetization at selected magnetic field strengths for polycrystalline **Gd**. The turquoise solid lines are the best fit as described in the main text.

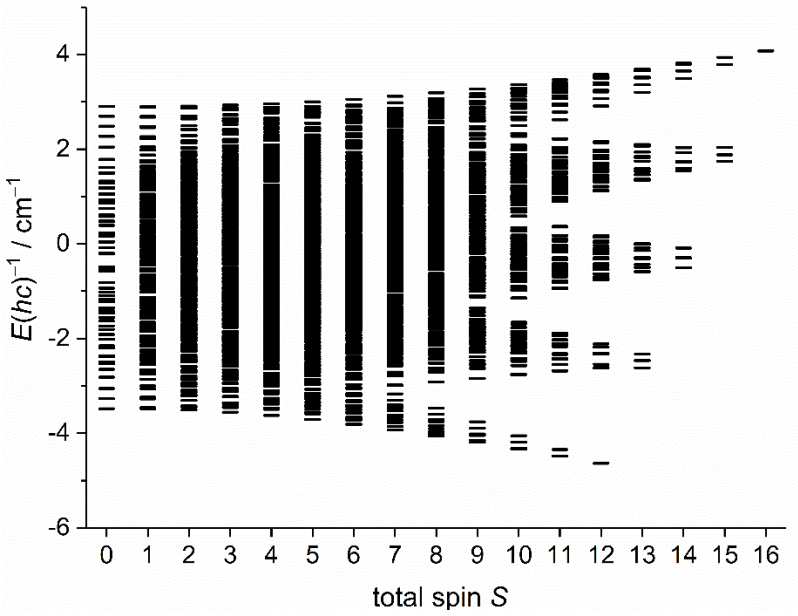

Fig. S8. Energy level spectrum of **Gd** determined as described in the main text.

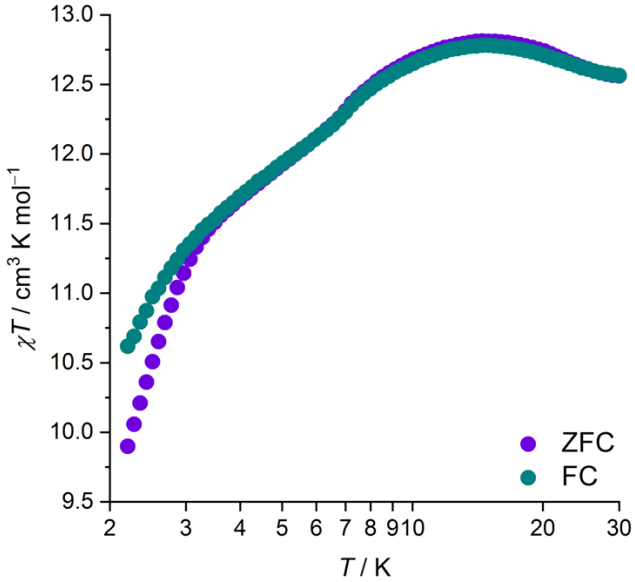

Fig. S9. Field-cooled (FC, 1000 Oe) and zero-field-cooled (ZFC) magnetization data plotted as χT vs T and obtained in heating mode with a magnetic field of $\mu_0 H$ = 1000 Oe.

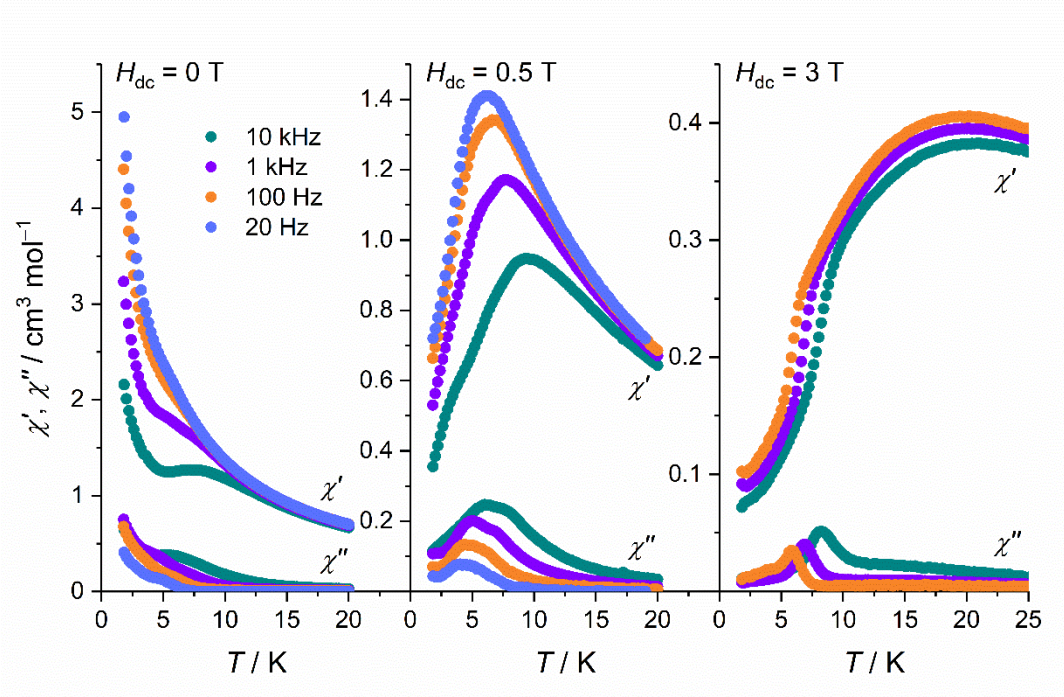

Fig. S10. Temperature dependence of the in-phase (χ') and out-of-phase (χ'') components of the ac susceptibility for polycrystalline **Dy** obtained with selected ac driving frequencies and in static (dc) fields of 0 T, 0.5 T, and 3 T.

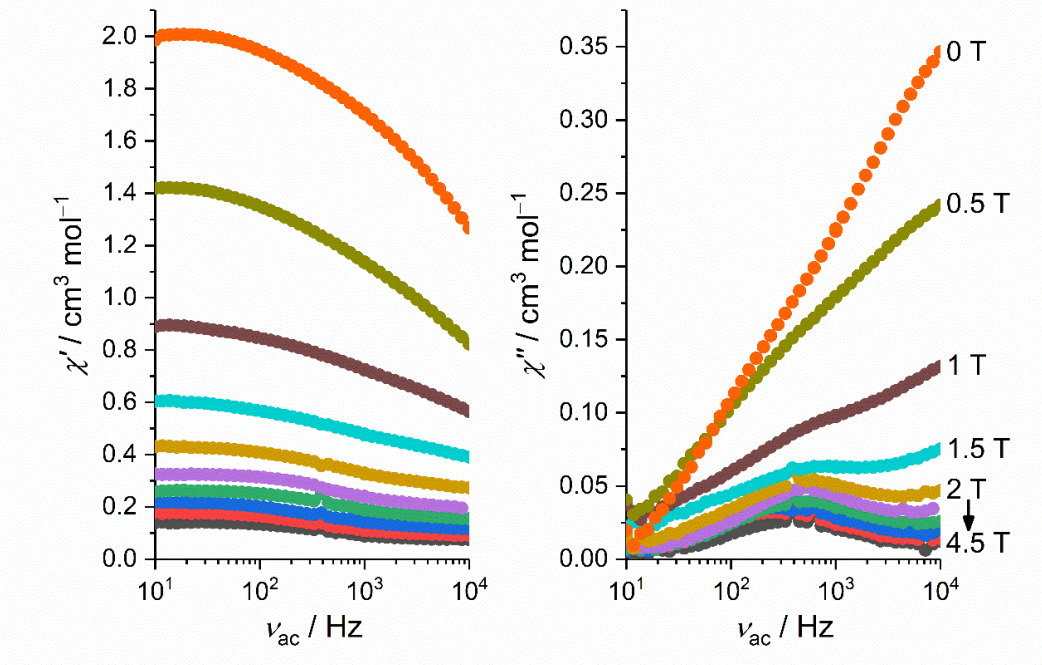

Fig. S11. Frequency dependence of the in-phase (χ', left) and out-of-phase (χ'', right) components of the ac susceptibility for polycrystalline **Dy** obtained in selected static (dc) fields at T = 6.5 K.

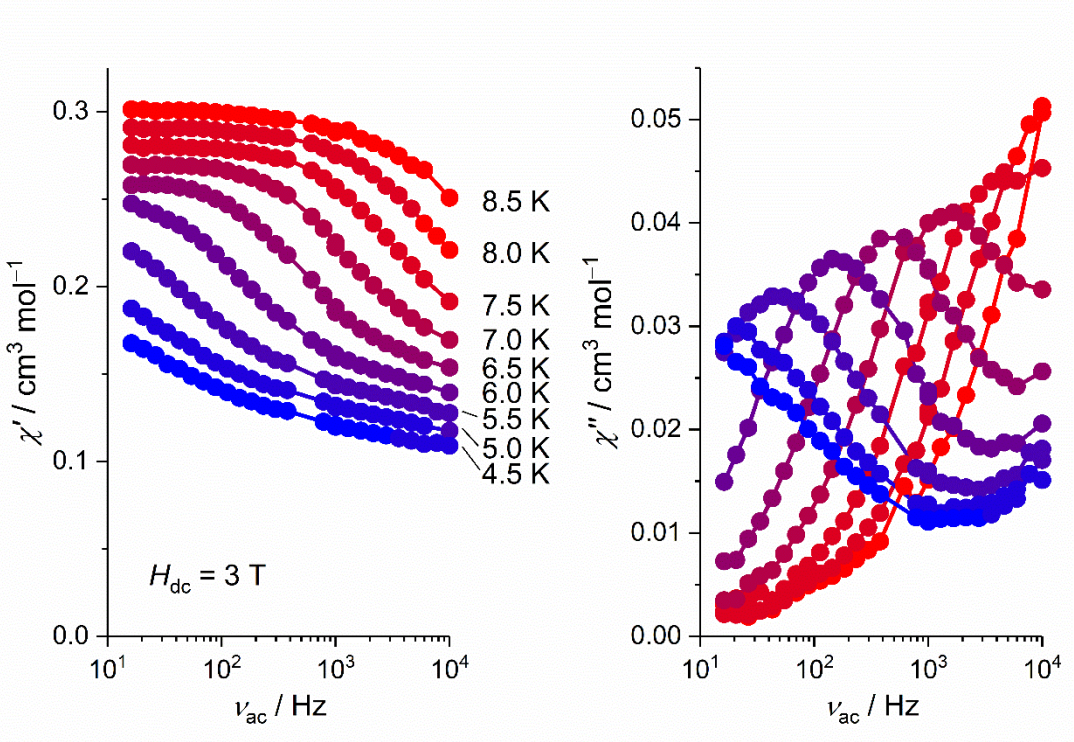

Fig. S12. Frequency dependence of the in-phase (χ', left) and out-of-phase (χ'', right) components of the ac susceptibility for polycrystalline **Dy** obtained at selected temperatures and in a static (dc) field of 3 T.

References

[1] O. V. Dolomanov, L. J. Bourhis, R. J. Gildea, J. A. K. Howard, H. Puschmann, *J. Appl. Cryst.* **2009**, *42*, 339-341.

[2] L. J. Bourhis, O. V. Dolomanov, R. J. Gildea, J. A. K. Howard, H. Puschmann, *Acta Cryst.* **2015**, *A71*, 59-75.

[3] G. M. Sheldrick, SHELXT-2018/2, Göttingen, Germany 2018.

[4] G.M. Sheldrick, *Acta Cryst.* **2015**, *C71*, 3-8.

[5] D. Kratzert, I. Krossing, *J. Appl. Cryst.* **2018**, *51*, 928-934.

[6] D. Kratzert, J. J. Holstein, I. Krossing, *J. Appl. Cryst*. **2015**, *48*, 933-938.

[7] B. L. Silver, Irreducible tensor methods: an introduction for chemists; Academic: New York, 36 **1976**.

[8] E. Anderson, LAPACK Users's Guide; 2nd ed.; Society for Industrial and Applied Mathematics: Philadelphia **1995**.

[9] W. H. Press, *et al.* Numerical recipes: the art of scientific computing; Cambridge University Press: Cambridge **1992**.